

Dynamic Light Scattering from Block Copolymer Solutions under the Zero Average Contrast Condition

Z. Liu, C. Pan,[†] and T. P. Lodge*

Department of Chemistry, University of Minnesota, Minneapolis, Minnesota 55455-0431

P. Stepanek

Institute for Macromolecular Chemistry, Czech Academy of Sciences, Prague, Czech Republic

Received December 2, 1994; Revised Manuscript Received February 23, 1995*

ABSTRACT: Dynamic light scattering measurements on a symmetric polystyrene–polyisoprene diblock copolymer, $M_w = 3.4 \times 10^5$, dissolved in neutral good solvents are reported. The solvents comprise mixtures of toluene and α -chloronaphthalene, and the solvent compositions necessary to index-match the entire copolymer, the polystyrene block, and the polyisoprene block have been determined. The first of these, the zero average contrast (ZAC) condition, is particularly advantageous as it eliminates the cooperative diffusion mode, thus enhancing the relative amplitude of the elusive internal mode. However, the ZAC condition is sensitive to small changes in either solvent composition or temperature. In dilute and semidilute ZAC solutions, the correlation functions consistently show two modes. The slower mode is diffusive, with a diffusivity in close agreement with that measured by pulsed-field-gradient NMR; it is thus interpreted as the heterogeneity mode, which is visible due to chain-to-chain variations in composition. The faster mode is the internal mode, with a decay rate that is independent of scattering angle and decreasing with concentration; the concentration dependence is that observed for the viscoelastic longest relaxation time. For polymer concentrations within a factor of 2 of the order–disorder transition, the total scattered intensity increases markedly, which is attributed to the appearance of large-amplitude concentration fluctuations. It is also shown that in dilute solution, the heterogeneity and cooperative modes have comparable decay rates, which can complicate the interpretation of the diffusional second virial coefficient, k_d , for copolymers.

Introduction

Block copolymer solutions exhibit rich structural and dynamic properties. The order–disorder transition (ODT) induced by the thermodynamic interactions between blocks, the variety of morphologies in the ordered state, micellization resulting from solvent selectivity, and strong concentration fluctuations in the disordered state near the ODT render the dynamics of block copolymer solutions both complicated and interesting.

Dynamic light scattering (DLS) is a powerful tool for the study of dynamics of polymer liquids. DLS senses the spontaneous concentration fluctuations in the system, with an intensity related to the corresponding optical contrast. This is particularly useful for block copolymers, since the presence of three chemical units (*i.e.*, solvent and two monomers) can serve to “label” multiple modes of relaxation of the concentration fluctuations, which might not be discernible for a homopolymer solution. Consequently, a single measurement by DLS may resolve several relaxation modes.

In this paper, we are concerned only with neutral (*i.e.*, nonselective) good solvents and symmetric diblock copolymers; such systems have been examined previously.^{1–8} Recent theories predict three relaxation modes in the intensity autocorrelation function measured by dynamic light scattering from such diblock copolymer solutions,^{7,9} which we designate the cooperative, internal, and heterogeneity modes. The first reflects the local concentration fluctuations of polymer relative to solvent, *i.e.*, mutual diffusion, and is consequently identical to that observed in homopolymer

solutions. The associated decay rate, Γ_C , is proportional to q^2 , where q is the scattering vector, and should scale with polymer concentration, c , and molecular weight, M , as $\Gamma_C \sim c^{0.75} M^0$ in the good solvent semidilute regime. The second mode arises from the relative motion of the different blocks; consequently, the decay rate, Γ_I , is independent of q (for $qR_g \ll 1$) and should be determined by the longest viscoelastic relaxation time of the chain. These two modes arise naturally in the linear response theory of Benmouna, Akcasu, *et al.*^{10–13} However, the heterogeneity mode, also called the polydispersity mode, arises from chain-to-chain variations in chemical composition, which can create composition fluctuations of arbitrary wavelength. For $qR_g \ll 1$, such fluctuations decay by exchange of A-rich and B-rich copolymers, and consequently the associated diffusion coefficient, $D_H = \Gamma_H/q^2$, reflects the translational diffusion of the copolymers. The resulting expression for the dynamic structure factor can therefore be written

$$\frac{S(q,t)}{S(q,0)} = A_C \exp(-\Gamma_C t) + A_I \exp(-\Gamma_I t) + A_H \exp(-\Gamma_H t) \quad (1)$$

assuming that the three modes are uncoupled.

Experimental evidence for all three modes was presented in two recent papers;^{7,8} in both cases the system was polystyrene–polyisoprene (PS–PI) in toluene. Furthermore, it was argued that eq 1 could reconcile all of the seemingly disparate observations of the earlier work.⁸ In refs 7 and 8, the cooperative mode was clearly resolved and shown to be identical to that observed in PS/toluene solutions. The correspondence of the heterogeneity mode to translational diffusion was also clearly shown for four different samples, by direct

* To whom correspondence should be addressed.

[†] Current address: Intel Corp., Santa Clara, CA 95052-8126.

© Abstract published in *Advance ACS Abstracts*, April 1, 1995.

comparison with self-diffusion measurements by pulsed-field-gradient NMR.⁸ The internal mode, however, has proven to be harder to characterize quantitatively. Generally, it has a lower amplitude than the other two, with $A_I \sim (qR_g)^2$, and particularly near the overlap concentration, $\Gamma_C \approx \Gamma_I$. Consequently, it can be difficult to resolve the internal mode by the standard Laplace inversion methods.

One promising approach is to employ a zero average contrast (ZAC) solvent, which in principle suppresses the cooperative mode completely, as noted by Benmouna *et al.*¹³ The average refractive index increment of the block copolymer in solution can be expressed as

$$\frac{dn}{dc} = f \left(\frac{\partial n}{\partial c} \right)_A + (1 - f) \left(\frac{\partial n}{\partial c} \right)_B \quad (2)$$

where (dn/dc) , $(\partial n/\partial c)_A$, and $(\partial n/\partial c)_B$ are the refractive index increments of the copolymer and of the A and B blocks and f is the weight fraction of A in the copolymer. At the ZAC condition for a symmetric block copolymer ($f = 0.5$), the refractive index increment of block A matches that of block B but is of opposite sign, and dn/dc vanishes. Since $A_C \sim (dn/dc)^2$, the cooperative mode disappears. Use of the ZAC condition has been reported for DLS studies of ternary systems^{14,15} and for neutron spin-echo studies of a PS-perdeuterio-PS diblock.^{16,17}

In this paper, we describe DLS measurements from block copolymer solutions under the ZAC condition. The polymer is a symmetric PS-PI diblock with total molecular weight 3.4×10^5 . The concentrations range from dilute to semidilute and up to the ODT. A mixed solvent of toluene and α -chloronaphthalene has been selected. An advantage of the mixed solvent is the ability to vary $\partial n/\partial c$ for each block continuously; thus the ZAC, zero contrast for the PS block (ZPS), and zero contrast for the PI block (ZPI) conditions can all be achieved. To assess the solvent quality as a function of solvent composition, intrinsic viscosities of the block copolymer in the mixed solvents were examined. An interferometric differential refractometer was employed to determine the zero contrast conditions. DLS results from ZPS and ZPI solutions are compared with those from ZAC solutions and with those reported previously in toluene,⁸ and finally the experimental results are compared with the recent theories.

Experimental Section

Samples and Solutions. A symmetric polystyrene-polyisoprene diblock copolymer with $M_w = 3.4 \times 10^5$ and $M_w/M_n = 1.08$ was employed; the polystyrene weight fraction was 0.50. This sample was previously examined extensively by dynamic light scattering in other solvents;⁸ it was designated SI(170-170). Spectrograde toluene from Fisher was used as received; α -chloronaphthalene with a purity of 99% was purchased from Kodak Laboratory Chemicals and was vacuum distilled near 112 °C under an absolute pressure of 5 mmHg. Mixed solvents with varying compositions of toluene were prepared gravimetrically. Both solvents were filtered through 0.2 μ m filters prior to mixing. Dilute solutions were prepared directly and filtered through 0.45 μ m filters into dust-free light scattering cells, and the cells sealed. Concentrated solutions were prepared as reported previously.⁸ A polystyrene homopolymer, $M_w = 1.52 \times 10^5$, from Pressure Chemical and a polyisoprene homopolymer, $M_w = 3.45 \times 10^4$, from Polymer Laboratories were used for the refractive index matching measurements. Deuterated chloroform (99.8%) from Cambridge Isotope Laboratories was used for the NMR measurements.

Intrinsic Viscosity. Viscosity measurements were performed in a thermostated water bath with Cannon-Ubbelohde semimicro dilution viscometers. The temperature was con-

trolled at 25.10 ± 0.01 °C. Five different solvent compositions, varying from pure α -chloronaphthalene to pure toluene, were covered. Intrinsic viscosity values were obtained by plotting η_{sp}/c and $\ln(\eta_r)/c$ against c and extrapolating to zero concentration. For all measurements, the extrapolated lines intersected at zero concentration.

Refractive Index Increment Measurements. A home-built differential refractometer was employed to estimate the zero average contrast conditions for the block copolymer and for the individual blocks. The design of this interferometric apparatus is similar to that available commercially from Wyatt Technology.¹⁸ A linearly polarized beam from a 5 mW He-Ne laser (Melles Griot) was resolved into two orthogonally polarized beams by a Wollaston prism, which were rendered parallel with a separation of 2.5 cm by a lens.¹⁹ The two beams then passed through two matched spectrophotometer cells (NSG), both firmly positioned in a temperature-controlled copper block. The two emerging beams were recombined and recollimated by an identical lens and prism assembly. A quarter-wave plate (with fast axis oriented parallel to the initial plane of polarization) then produces linearly polarized light, with the orientation angle of the polarization governed by the phase retardation φ between the two beams. After passing through an analyzing polarizer, the transmitted light was detected by a photodiode. Intensity measurements were made at 10° increments by rotating the analyzer, and the resulting data were fit to a sine function to obtain the phase ψ . The phase retardation between the two light waves is

$$\varphi = \frac{2\pi L \Delta n}{\lambda_0} \quad (3)$$

where $\Delta n = n_s - n_r$ is the difference between the refractive indices of the reference liquid and sample, λ_0 is the wavelength of incident light, and L is the path length of the sample cells. Given that $\varphi = 2\psi$, Δn can be determined directly. Equation 3 assumes that all other sources of phase retardation between the two paths are held constant.

In principle, this refractometer has a sensitivity of at least 10^{-7} , which is advantageous for determining small values of dn/dc . To measure $\Delta n/\Delta c$ for a particular solvent composition, a series of samples ranging from solvent to a polymer solution with weight fraction $c \approx 0.01$ were prepared.²⁰ The solvent was used in both cells to determine the initial phase angle, ψ_0 . Then, the solvent was replaced in one cell by the solution of lowest concentration, and a measurement taken. Subsequent readings were obtained by alternating which cell was filled with the new solution, to keep Δn approximately constant during the measurement series. The ZAC condition at 30.0 °C was examined by varying solvent composition around 0.48 in toluene weight fraction. The ZPS and ZPI conditions were similarly determined with solutions containing PS and PI homopolymers. Each value of $\Delta n/\Delta c$ reflects the average of measurements on four polymer solutions. In addition, the refractive indices of the mixed solvent were examined as a function of solvent composition with an Abbé refractometer (Carl Zeiss Jean).

Dynamic Light Scattering Measurements. The DLS apparatus was described previously.⁸ The light source is a Spectra-Physics 165 Ar⁺ laser operating at 488 nm. The time autocorrelation functions of the scattered intensity $g^{(2)}(q, \tau)$ were accumulated in the homodyne mode using a 264-channel multi-sample time autocorrelator (BI-2030AT from Brookhaven Instruments). For each solution, $g^{(2)}(q, \tau)$ was obtained at seven scattering angles from 45 to 135°, and the decays reached the calculated baseline to within 0.1% in all cases. The correlation functions were analyzed by the inverse Laplace transform program CONTIN.²¹ All measurements were performed at a temperature of 30.0 ± 0.1 °C, unless otherwise indicated.

Pulsed-Field-Gradient NMR Measurements. Solutions were prepared in deuterated chloroform and flame-sealed under vacuum in regular NMR tubes. Samples were stored for more than 1 month before use. Measurements were performed at 30.0 ± 0.5 °C on an NT-300 instrument from Nicolet Magnetics Corp. The pulse sequence can be expressed as $90^\circ(\text{rf}) - t_1 - \delta(\text{FG}) - t_2 - 180^\circ(\text{rf}) - t_1 - \delta(\text{FG}) - t_2 -$

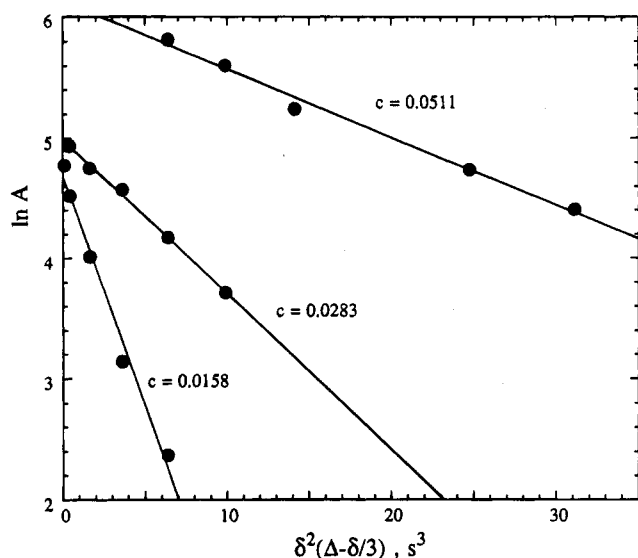


Figure 1. Attenuation of spin-echo intensity for SI(170-170) in CDCl_3 at the indicated polymer concentrations.

echo.^{22,23} The time interval $\Delta = t_1 + \delta + t_2$ is held constant, while δ is automatically incremented and t_2 is decreased at each same step. The attenuated spin-echo signal intensity, A , is related to the molecular self-diffusion coefficient, D_s , by the equation

$$A = A(0) \exp\left(-\frac{2\Delta}{T_2}\right) \exp\left[-\gamma^2 G^2 D_s \delta^2 \left(\Delta - \frac{\delta}{3}\right)\right] \quad (4)$$

where T_2 is the spin-spin relaxation time, γ is the gyromagnetic ratio of the proton, and G is the field gradient strength.^{22,23} The slope of a plot of $\ln(A)$ vs $\delta^2(\Delta - \delta/3)$ thus allows one to determine either D_s if G is known or G if D_s is known; examples are shown in Figure 1. In this case, benzene ($D_s = 2.28 \times 10^{-5} \text{ cm}^2/\text{s}$ at 25°C) was employed to calibrate G . As these measurements were made in the Fourier transform mode, it is possible in principle to select any of several spectrally distinct protons for the measurement. However, it is advantageous to choose one with a large T_2 , and consequently the methyl and methylene protons with a chemical shift of ca. 1.7 ppm were selected.

Results and Discussion

The remainder of the paper is organized as follows. First we discuss the characterization of the mixed solvent. Second, we consider the DLS results in dilute solutions, varying mean solvent refractive index through solvent composition and, in one instance, by temperature. We demonstrate the effectiveness of the ZAC condition for characterizing the internal mode and confirm the coincidence of the cooperative mode and the heterogeneity mode relaxation rates in this regime. We also point out that this latter phenomenon complicates the interpretation of the diffusional second virial coefficient, k_d , obtained for block copolymers. Then we describe measurements through the semidilute regime and up to the ODT.

Characterization of the Mixed Solvent. The two solvents are miscible in all proportions, and toluene is a good solvent for both polymers; α -chloronaphthalene is a good solvent for polystyrene, and, based on solubility parameters, we expect it to be somewhat less good for polyisoprene. This mixture was employed previously by Chu and Wu to examine solution blends of polystyrene and poly(methyl methacrylate), with no anomalous results reported.²⁴ The refractive index of the mixed solvent is shown in Figure 2a as a function of toluene

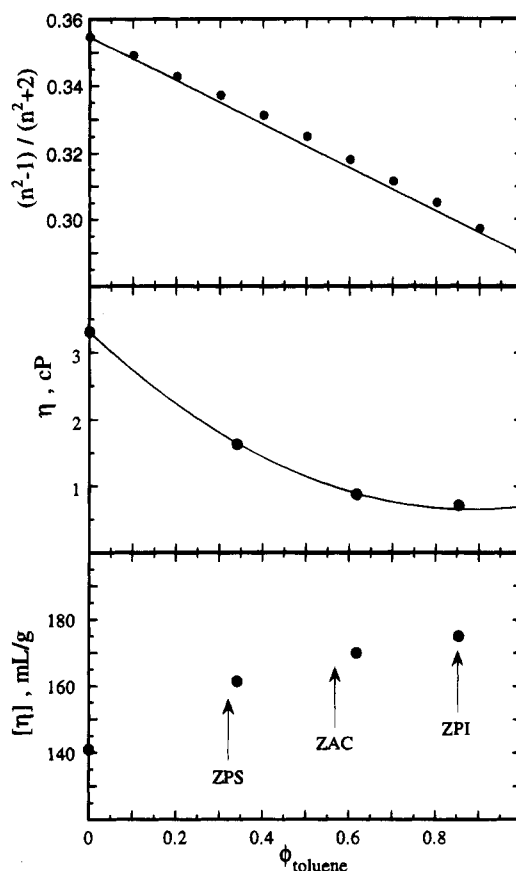


Figure 2. Characterization of toluene/ α -chloronaphthalene mixtures: (a) refractive index, (b) viscosity, and (c) intrinsic viscosity of SI(170-170) as a function of toluene volume fraction in the mixed solvent.

volume fraction, ϕ_{tol} . The straight line corresponds to the prediction of the Lorentz-Lorenz equation,²⁵ assuming no volume change upon mixing; the data deviate from this relation only slightly. The viscosity of the mixed solvent, η , is shown in Figure 2b, with the smooth curve corresponding to the empirical relation $\eta = 3.31 - 6.03\phi_{\text{tol}} + 3.42\phi_{\text{tol}}^2$. These data were obtained with a capillary viscometer, and the density of the mixed solvent was calculated assuming no volume change on mixing. The principal feature to note is that η varies by less than a factor of 3 over the range from neat toluene to the ZPS condition.

The most important issue is whether the effective solvent quality or neutrality varies significantly over the relevant composition range. In Figure 2c the intrinsic viscosity of the copolymer is plotted versus solvent composition. Although $[\eta]$ is noticeably lower in pure α -chloronaphthalene than in pure toluene, most of the variation occurs when $\phi_{\text{tol}} < 0.3$, which is outside the range of the DLS measurements. Over the relevant range, from pure toluene to ZPS, $[\eta]$ decreases by less than 10%, which reflects a decrease in R_g of only about 3%. Consequently, within the precision of the DLS measurements, we can take the mixed solvents to be of equivalent quality. The fact that $[\eta]$ lies above an "ideal mixing" linear interpolation between the values in the neat solvents suggests some preferential solvation. However, this is not of any particular concern here, because (i) we still determine the ZAC condition directly for the copolymer and (ii) we are not using light scattering intensities to extract molecular weight information. There could well be some differential preferential solvation, e.g., toluene preferentially solvates

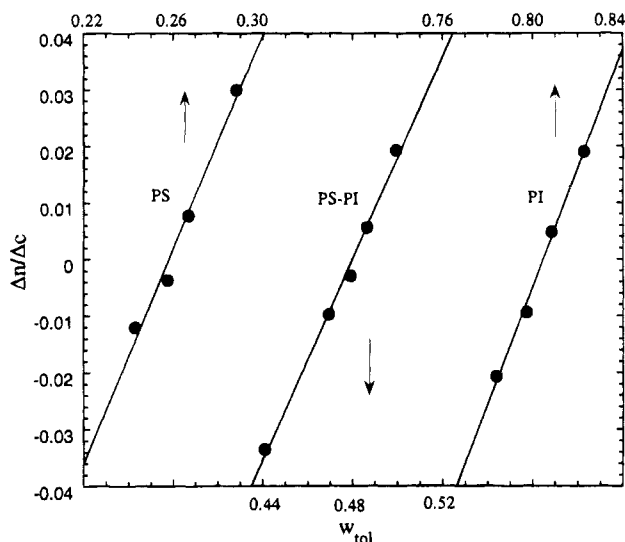


Figure 3. Variation of refractive index increment for polystyrene homopolymer, SI(170–170), and polyisoprene homopolymer in toluene/α-chloronaphthalene mixtures as a function of toluene weight fraction in the mixed solvent.

both blocks, but to different extents, but it is unlikely that this exerts a significant effect on the behavior of the copolymer. Evidence in support of this comes from static birefringence measurements. For this polymer in toluene, the ODT at 30 °C occurs for $c = 0.14$.²⁶ ZAC solutions with $c = 0.12$ and 0.14 were disordered and ordered, respectively, at room temperature, and consequently the ZAC solvent is close to toluene in a thermodynamic sense.

The determination of the ZAC, ZPS, and ZPI conditions is illustrated in Figure 3, where $\Delta n/\Delta c$ is plotted as a function of the weight fraction of toluene, w_{tol} , in the mixed solvent. (The weight fraction is employed here because that is the experimentally determined composition variable.) The resulting values at 30 °C are $w_{\text{tol}} = 0.480$ (ZAC), 0.258 (ZPS), and 0.804 (ZPI). In all three cases $\Delta n/\Delta c$ varies smoothly, albeit rapidly, with w_{tol} . We attribute the major source of uncertainty to the determination of w_{tol} and polymer concentration, given the different evaporation rates of the two solvents. As noted in the Experimental Section, $\Delta n/\Delta c$ was obtained as an average from four polymer solutions and the neat solvent, with no polymer concentration dependence evident; thus we can ignore the technicality that $\Delta n/\Delta c$ is not obtained at constant chemical potential of either solvent component. However, we cannot be certain that the ZAC composition thus determined will be precisely the ZAC condition in a concentrated polymer solution. It should also be pointed out that the ZPS and ZPI conditions may also not be exact for the block copolymer, as dn/dc may vary slightly with differences in microstructure and molecular weight between the diblock and the homopolymers.

Dilute Solution Results. Our previous measurements in toluene demonstrated that in the limit $c \rightarrow 0$, $\Gamma_C = \Gamma_H$.⁸ Consequently, one expects to observe two peaks in the inverse Laplace transform (ILT), one with amplitude $A_C + A_H$ and one with amplitude A_I . In terms of scattering contrast, both A_H and A_I are predicted to scale with the difference in scattering power between the PS and PI blocks, whereas A_C depends on dn/dc for the copolymer.^{7,9,13} Thus, as the solvent refractive index is varied, $A_I/(A_C + A_H)$ should exhibit a maximum at the ZAC. This is illustrated in Figure 4 for a solution with $c = 0.00220$ and a scattering angle of 90°. The

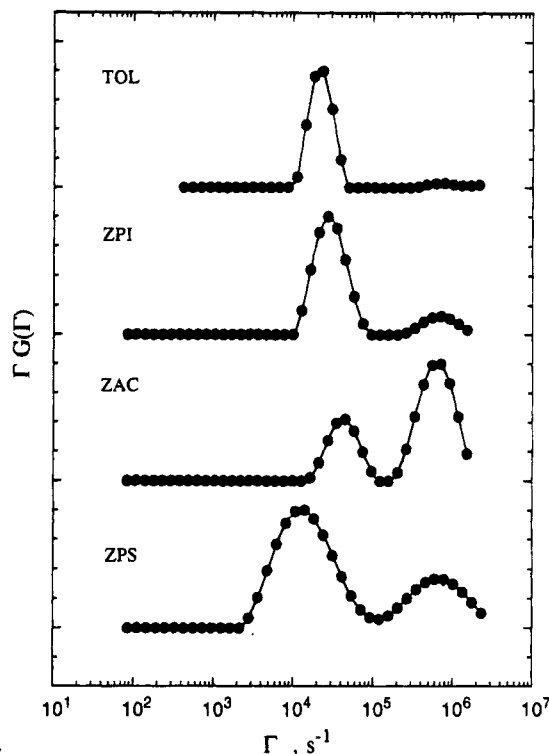


Figure 4. Inverse Laplace transforms of the measured intensity correlation functions (in the equal-area representation) for dilute SI(170–170) solutions ($c \approx 0.002$) as a function of solvent composition at a scattering angle of 90°.

slower mode, which completely dominates the ILT in toluene, corresponds to the combined cooperative and heterogeneity modes, whereas the faster mode, which is most apparent in the ZAC solution, is assigned to the internal mode. The remaining amplitude in the slower mode for the ZAC solution can be attributed to A_H , but not in its entirety. The reason is important to note: the compositional heterogeneity that gives rise to A_H necessarily means that A_C cannot be exactly zero, even in a ZAC solvent. In other words, the ZAC condition (*i.e.*, eq 2 equals zero) applies to the copolymer solution *as a whole*, but not to every single chain. Two other features in Figure 4 require comment. First, the peak widths vary somewhat with solvent contrast, and second, the position of the slow mode varies with solvent composition, but not monotonically with solvent viscosity. We attribute both observations to inherent uncertainty in the ILT of multimodal correlation functions. This well-known difficulty is exacerbated in Figure 4 by the very small scattered intensity, resulting from the low polymer concentration and the ZAC condition. For example, the first channels in the normalized intensity correlation functions range from only *ca.* 1.02 in the ZAC solution to 1.045 in the ZPI solution.

The angle dependences of the two modes in the ZAC solution are illustrated in Figure 5; Γ_H varies linearly with q^2 whereas Γ_I is independent of q . These angle dependences will be demonstrated more quantitatively subsequently. The temperature dependence of the two modes in the ZAC solution is pictured in Figure 6a; also indicated is the temperature dependence of the total scattered intensity. Simply by moving 10 deg above or below 30 °C, the relative amplitude of $A_H + A_C$ increases markedly; Figure 6b plots the two amplitudes directly. The distinct minimum near 30 °C indicates that the difference in wavelength between the refractometer and the DLS laser is of little consequence in determining

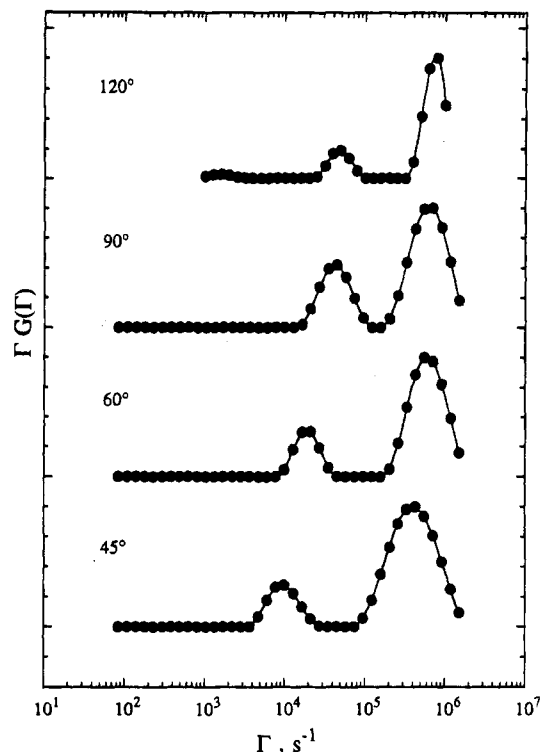


Figure 5. Angle dependence of the inverse Laplace transforms for a dilute SI(170-170) solution, $c = 0.00220$, in the ZAC solvent.

the ZAC composition. The comments about the peak positions and widths in Figure 4 apply also to Figure 6a.

The data in Figure 6 demonstrate that the exact ZAC composition for a given copolymer is a sensitive function of temperature. It is also the case that the ZAC condition is a sensitive function of composition at fixed temperature, as illustrated in Figure 7. Here, ILTs for dilute solutions with $c \approx 0.006$ – 0.008 and a scattering angle of 45° are shown for various solvent compositions. In particular, varying w_{tol} by 0.004 , i.e., by less than 1% of the ZAC composition, is sufficient to make $A_H + A_C > A_I$, whereas $A_H < A_I$.

The overlap of the cooperative and heterogeneity modes in dilute solution can affect the interpretation of the diffusional second virial coefficient, k_d . For homopolymers, k_d is extracted from dilute solution measurements via the relation

$$D_C = D_0(1 + k_d c + \dots) \quad (5)$$

where D_C is the measured mutual diffusion coefficient and D_0 is the translational diffusion coefficient of the polymer at infinite dilution. To the extent that the heterogeneity mode reflects translational diffusion, the analogous expansion would be

$$D_H = \frac{kT}{\xi(c)} = D_0(1 - k_f c + \dots) \quad (6)$$

where $\xi(c)$ is the polymer friction coefficient. For homopolymers,

$$k_d = 2A_2M - k_f - v \quad (7)$$

where A_2 is the osmotic second virial coefficient and v is the partial specific volume of the polymer.²⁷ If one were to interpret the overlapping cooperative and

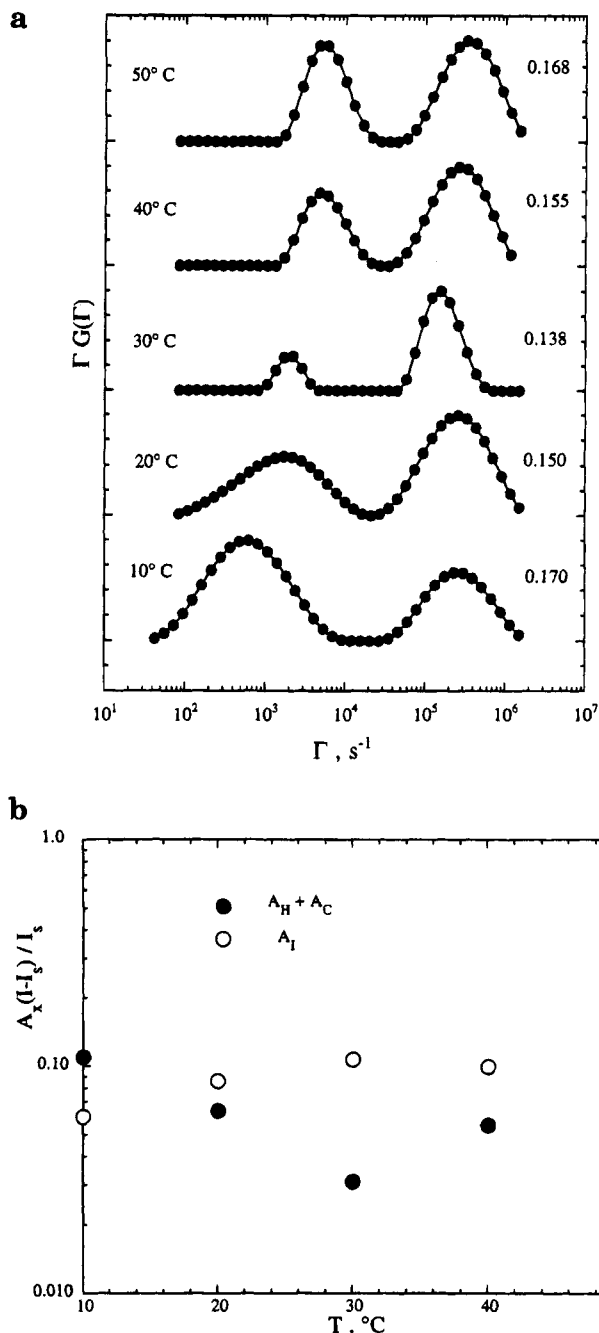


Figure 6. Temperature dependence of (a) the inverse Laplace transform and (b) amplitude of the heterogeneity and internal modes for the same solution as in Figure 5 at a scattering angle of 45° . The fractional amplitudes in (b) are multiplied by the excess scattered intensity relative to the pure solvent, $(I - I_s)/I_s$; the corresponding values of $(I - I_s)/I_s$ are listed in (a).

heterogeneity modes in a block copolymer as due to cooperative diffusion alone, the resulting apparent value of k_d would be

$$k_d^{\text{app}} = 2\beta A_2M - k_f - \beta v \quad (8)$$

where β is the fractional amplitude of the cooperative mode. Thus, the apparent k_d would be less than the true k_d , because $\beta < 1$ and $A_2 > 0$ in a good solvent. Fortunately, the results in Figures 4, 6a, and 7 suggest that β will be close 1 unless one is close to the ZAC condition.

Concentration Dependence. The ILTs of four semidilute solutions of SI(170-170) with different solvent compositions are shown in Figure 8 at a scattering

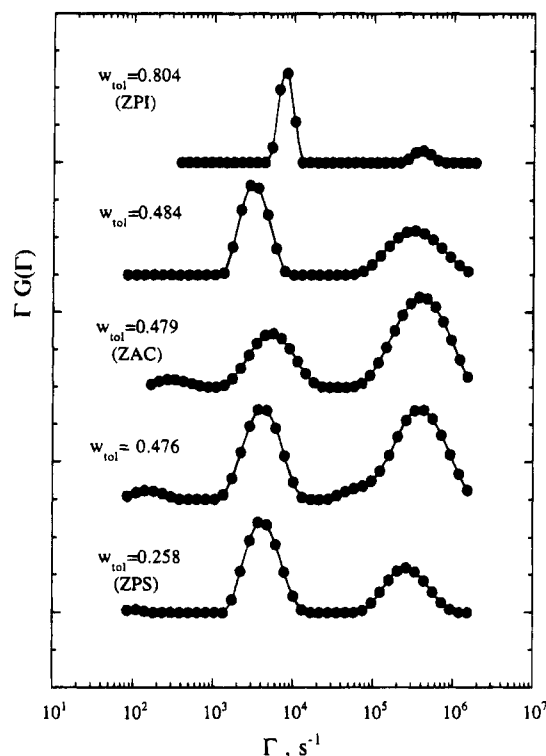


Figure 7. Inverse Laplace transforms for dilute SI(170–170) solutions, $c \approx 0.006$ – 0.008 , as a function of solvent composition near the ZAC condition at a scattering angle of 45° .

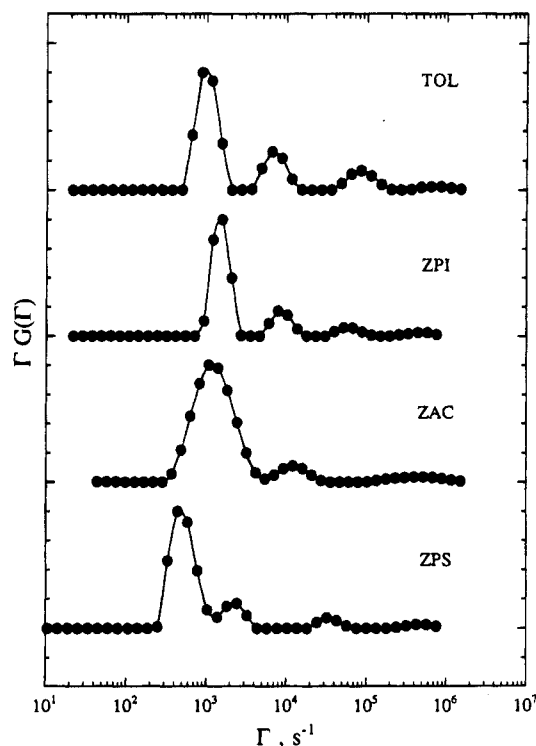


Figure 8. Inverse Laplace transforms for semidilute SI(170–170) solutions, $c \approx 0.06$, as a function of solvent composition at a scattering angle of 90° .

angle of 90° . The four polymer concentrations vary slightly, but this does not obscure the main features. All four inversions are dominated by the slow mode, which corresponds to Γ_H . The ZAC solution shows one small, faster mode, attributed to Γ_I , whereas the other three solvents show small but distinct third peaks at higher frequencies. These are assigned to the cooperative mode, which becomes visible as the ZAC condition

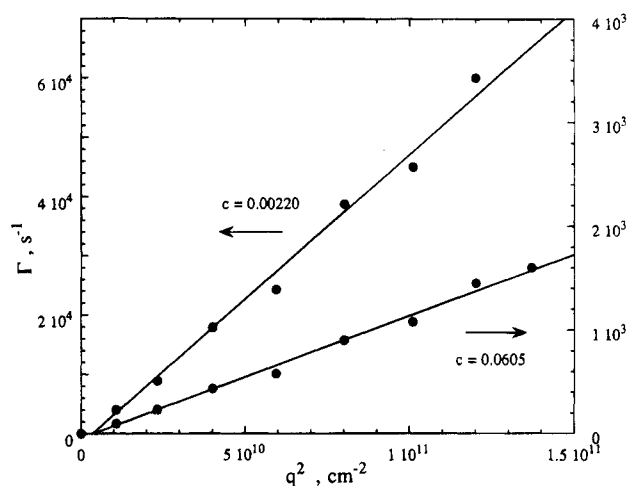


Figure 9. Angle dependence of Γ_H in a dilute ($c = 0.00220$) and a semidilute ($c = 0.0605$) ZAC solution.

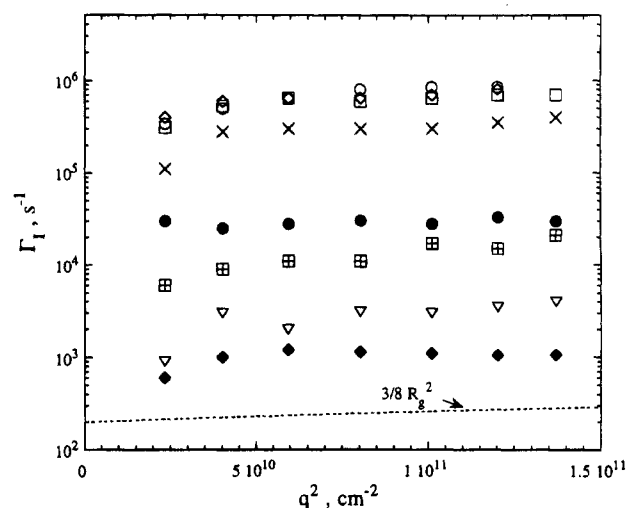


Figure 10. Angle dependence of Γ_I in ZAC solutions as a function of concentration; from top to bottom the data correspond to $c = 0.00220, 0.00703, 0.00830, 0.0130, 0.0544, 0.0605, 0.0753$, and 0.118 . The predicted q dependence corresponding to eq 9 is shown as the smooth curve.

is relaxed. The measurements in toluene were reported previously, and the assignment of the cooperative and heterogeneity modes was clearly confirmed by both the absolute magnitude and the q^2 dependences of the respective decay rates.⁸ It is interesting to note that the peak attributed to Γ_I appears to move around from solvent to solvent more than can be accounted for by changes in solvent viscosity. For example, Γ_I appears to be about a factor of 5 greater in the ZAC solution than in the ZPS. As before, we are inclined to attribute this to uncertainties in the ILT, particularly when the number of modes differs. For the ZAC solution, the breadth of the Γ_H peak is substantially larger than in the other three solutions, which is presumably not physically significant.

The angle dependence for Γ_H in ZAC solutions is illustrated in Figure 9, for the dilute solution shown in Figure 5 and the semidilute solution in Figure 8; the q^2 dependence establishes the diffusive origin of this mode. The angle dependence of the mode assigned to Γ_I is shown in Figure 10 for eight solutions extending from the dilute regime to near the ODT, and including those in Figures 5 and 8. Clearly, Γ_I is essentially independent of q , although the lowest angle data appear to be slightly lower than the others; this is due, at least in

part, to the fact that A_I is predicted to increase with q and that thus the lowest angle points are the least reliable. The theory of Benmouna *et al.* leads to a quantitative prediction for the q dependence of Γ_I when the condition $qR_g \ll 1$ is relaxed, assuming high molecular weight, Gaussian, Rouse chains in dilute solution:^{8,12,13}

$$\Gamma_I = \frac{6kT}{N\zeta_0 R_g^2} \left(1 + \frac{3}{8} q^2 R_g^2 + \dots \right) \quad (9)$$

where N is the degree of polymerization and ζ_0 is the monomeric friction coefficient. This prediction is shown on Figure 10, assuming $R_g = 28.4$ nm. The agreement is reasonable within the uncertainty, but in general the q dependence is weaker than predicted; this could be a consequence of hydrodynamic interactions, which tend to decrease the q dependence of relaxation rates of internal modes. The concentration dependence of the $q = 0$ intercept is identical to that of D_H and D_s , as will be discussed subsequently.

Rey and Freire have recently presented an analysis of $S(q, t)$ for an isolated symmetric diblock copolymer in a ZAC solvent.²⁸ Their treatment, as it considers an ideal copolymer, naturally excludes the heterogeneity mode. However, they do predict a single-exponential decay under conditions comparable to those for our most dilute solutions. Interestingly, this decay incorporates both the internal mode and the diffusivity, *i.e.*, $\Gamma \approx q^2 D + \tau_1^{-1}$. However, the diffusive contribution would be too small to resolve for SI(170–170) over the accessible q range.

The concentration dependences of the intensity correlation functions and the corresponding ILTs are shown over the whole range of concentration for the ZAC solutions in Figures 11a and 11b, respectively. Also indicated in Figure 11a is the concentration dependence of the excess scattered intensity. To a good approximation, Γ_H and Γ_I have a similar concentration dependence, which is reasonable given that one reflects chain diffusion and the other the longest viscoelastic relaxation time, τ_1 . This is more evident in Figure 12, where D_H and Γ_I/q^2 (for $\theta = 90^\circ$) are plotted together. Also shown are the measurements of D_s in chloroform by NMR, confirming that $D_H \approx D_s$ (in the figure D_s has been scaled by the ratio of solvent viscosities). The concentration dependence of the internal mode has been modeled with

$$\Gamma_I^{-1} \propto \tau_1 \approx \tau_1^0 \exp(Ac[\eta]) \quad (10)$$

a semiempirical expression^{29–31} that has been shown to describe oscillatory flow birefringence, viscoelasticity, and dielectric relaxation data very well.^{32–36} The value of A obtained by the fit shown in Figure 12 is 0.46, in excellent agreement with the values between 0.4 and 0.5 obtained for polystyrenes ($M \geq 10^5$) in Aroclor^{32–35} and in good agreement with the value of 0.294 reported for polyisoprene in Isopar.³⁶ The value of τ_1^0 obtained is 1.5 μ s, which compares favorably to an estimate of 7 μ s, based on the Zimm model through the measured intrinsic viscosity.^{37,38}

Returning to Figure 11b, in all but the dilute solutions, the heterogeneity mode dominates, so in this case, even the virtual elimination of the cooperative mode has not served to allow complete characterization of the internal mode. The intensities of the two modes, A_I and A_H (multiplied by the excess scattered intensity), are

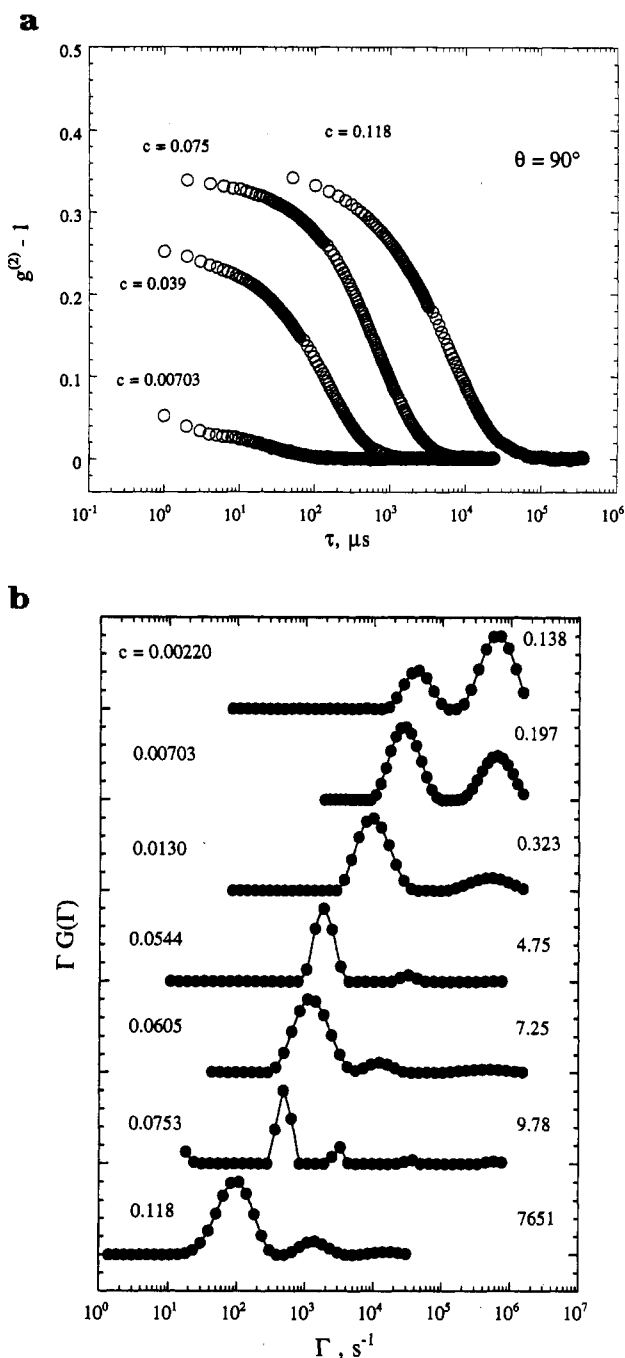


Figure 11. (a) Intensity correlation functions and (b) inverse Laplace transforms for SI(170–170) in ZAC solutions at the indicated concentrations at a scattering angle of 90° . The excess scattered intensity relative to the solvent, $(I - I_s)/I_s$, is also indicated in (b).

shown as a function of concentration in Figure 13. In dilute solution, $A_I > A_H$, but then A_H overtakes A_I near $c^* \approx 0.01$. The prediction for dilute solutions is that both A_I and A_H should increase linearly with c ,^{7,9,13} but only A_H follows this scaling. In the semidilute regime, Jian *et al.*^{7,9} predict that A_I scales as $c^{0.75}$, which is also not observed. Above $c \approx 0.05$, both A_I and A_H increase very strongly (note the logarithmic axes). In the mean-field prediction for A_H ^{7,9}

$$A_H \propto \frac{\kappa N c}{1 - 2\kappa \chi N c^{1.53}} \quad (11)$$

there is the possibility of a divergence at high concen-

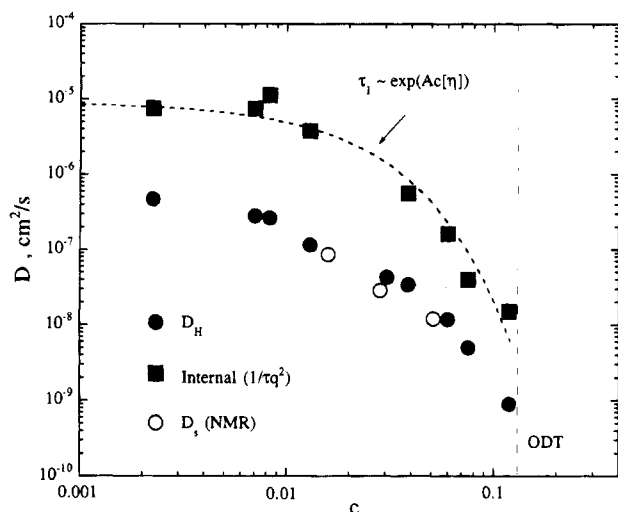


Figure 12. Concentration dependence of D_H and D_s from NMR and Γ_1/q^2 (at 90°) for SI(170–170) in the ZAC solvent. The vertical line denotes the order–disorder transition, and the dashed line a fit of Γ_1 to the exponential relation given in eq 10.

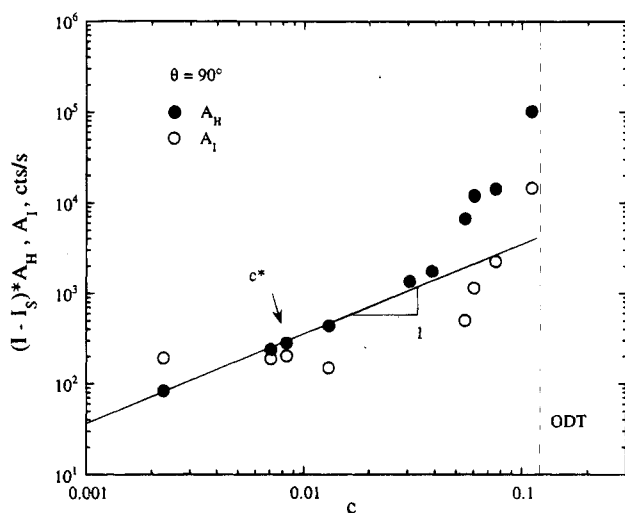


Figure 13. Concentration dependence of the fractional amplitudes of the heterogeneity and internal modes for SI(170–170) in the ZAC solvent multiplied by the excess scattered intensity, $(I - I_s)$.

tration, if the heterogeneity factor, κ , is sufficiently large:

$$\kappa \approx 2 \frac{M_w - M_n}{M_n} \frac{f^2(1-f)^2}{f^2 + (1-f)^2} \quad (12)$$

However, given that $\chi N c^{1.53} \approx 10$ at the ODT^{39,40} and that $\kappa \approx 0.02$ for SI(170–170), eq 11 cannot describe the strength of the observed increase in A_H . Furthermore, mean-field theory does not predict a divergence for A_I . Consequently, we are inclined to attribute this extra intensity to a non-mean-field effect, namely, the onset of large-amplitude composition fluctuations, as extensively documented for other disordered block copolymer systems near the ODT.^{41–43}

Summary

Dynamic light scattering from a symmetric polystyrene–polyisoprene diblock copolymer has been examined in dilute and semidilute solutions in mixed solvents containing α -chloronaphthalene and toluene. By vary-

ing the solvent composition, it was possible to achieve the zero average contrast (ZAC) condition, in which dn/dc for the average copolymer vanishes and also the conditions where $\partial n/\partial c$ for the individual blocks are masked. Intrinsic viscosity measurements were conducted to evaluate the mixed solvents, and the solvent quality remained essentially constant over the relevant range of solvent composition. Pulsed-field-gradient NMR was used to determine the self-diffusion coefficient of the copolymer in selected solutions. In general, the results both confirm and extend those recently reported for polystyrene–polyisoprene copolymers in toluene.^{7,8} The specific conclusions are as follows:

1. Under the ZAC condition, the cooperative diffusion mode was not observed, as expected. However, only small changes in solvent composition (e.g., 1%) or temperature (e.g., 10 deg) were required to produce significant amplitude in the cooperative mode.

2. Under the ZAC condition the correlation functions at all concentrations examined reflected two modes, which were interpreted as the heterogeneity and internal modes, with decay rates Γ_H and Γ_I and amplitudes A_H and A_I , respectively. The former mode is visible due to chain-to-chain variations in composition and reflects translational diffusion of the copolymer chains; the latter corresponds to intramolecular relaxation.

3. Throughout the examined concentration range, $\Gamma_H \sim q^2$, and the resulting diffusion coefficients were in good agreement with those from NMR. Concurrently, $\Gamma_I \sim q^0$ and displayed the concentration dependence expected for the longest viscoelastic relaxation time.

4. In dilute solution for non-ZAC solvents, it was shown that the heterogeneity mode and the cooperative mode overlap. If not recognized, this can lead to improper interpretation of the diffusional second virial coefficient, k_d , for block copolymers.

5. In dilute solution, $A_I > A_H$, but above coil overlap $A_H > A_I$. For concentrations within a factor of 2 of the order–disorder transition, the total scattered intensity increased markedly, as did A_H and A_I . This could not be described by the mean-field theories and is tentatively attributed to the onset of large-amplitude concentration fluctuations, as previously reported for copolymer melts and solutions.

Acknowledgment. This work was supported in part by the National Science Foundation, through Grants DMR-9018807 (T.P.L.) and CHE-9203173 from the NSF Division of International Programs (a U.S.–Czech Cooperative Research award, T.P.L. and P.S.). In addition, the work was supported by the Center for Interfacial Engineering, an NSF-supported Engineering Research Center at the University of Minnesota. The refractometer was constructed with the assistance of Dr. S. Amelar, and the NMR measurements were performed with the assistance of Dr. S. Philson. The willingness of Dr. H. Watanabe to provide the polymer sample is also gratefully acknowledged.

References and Notes

- (1) Balsara, N. P.; Stepanek, P.; Lodge, T. P.; Tirrell, M. *Macromolecules* **1991**, *24*, 6227.
- (2) Borsali, R.; Fischer, E. W.; Benmouna, M. *Phys. Rev. A* **1991**, *43*, 5732.
- (3) Duval, M.; Haida, H.; Lingelser, J. P.; Gallot, Y. *Macromolecules* **1991**, *24*, 6867.
- (4) Haida, H.; Lingelser, J. P.; Gallot, Y.; Duval, M. *Makromol. Chem.* **1991**, *192*, 2701.
- (5) Konak, C.; Podesva, J. *Macromolecules* **1991**, *24*, 6502.

- (6) Tsunashima, Y.; Kawamata, Y. *Macromolecules* **1993**, *26*, 4899.
- (7) Jian, T.; Anastasiadis, S. H.; Semenov, A. N.; Fytas, G.; Adachi, K.; Kotaka, T. *Macromolecules* **1994**, *27*, 4762.
- (8) Pan, C.; Maurer, W.; Liu, Z.; Lodge, T. P.; Stepanek, P.; von Meerwall, E. D.; Watanabe, H. *Macromolecules* **1995**, *28*, 1643.
- (9) Semenov, A. N.; Fytas, G.; Anastasiadis, S. H. *Polym. Prepr. (Am. Chem. Soc., Div. Polym. Chem.)* **1994**, *35*(1), 618.
- (10) Akcasu, A. Z.; Hammouda, B.; Lodge, T. P.; Han, C. C. *Macromolecules* **1984**, *17*, 759.
- (11) Akcasu, A. Z.; Benmouna, M.; Benoit, H. *Polymer* **1986**, *27*, 1935.
- (12) Benmouna, M.; Duval, M.; Borsali, R. *J. Polym. Sci., Polym. Phys. Ed.* **1987**, *25*, 1839.
- (13) Benmouna, M.; Benoit, H.; Borsali, R.; Duval, M. *Macromolecules* **1987**, *20*, 2620.
- (14) Giebel, L.; Benmouna, M.; Borsali, R.; Fischer, E. W. *Macromolecules* **1993**, *26*, 2433.
- (15) Borsali, R.; Duval, M.; Benmouna, M. *Macromolecules* **1989**, *22*, 816.
- (16) Borsali, R.; Benoit, H.; Legrand, J.-F.; Duval, M.; Picot, C.; Benmouna, M.; Farago, B. *Macromolecules* **1989**, *22*, 4119.
- (17) Duval, M.; Picot, C.; Benoit, H.; Borsali, R.; Benmouna, M.; Lartigue, C. *Macromolecules* **1991**, *24*, 3185.
- (18) Wyatt, P. J. *Anal. Chim. Acta* **1993**, *272*, 1.
- (19) The wavelength difference between the lasers in the refractometer and the dynamic light scattering spectrometer is assumed to be inconsequential in the subsequent analysis.
- (20) Polymer concentrations are expressed as weight fractions, with the symbol c . Weight fractions are employed because they are the experimentally determined quantities; the symbol c is used to avoid confusion with f , the weight fraction of styrene in the copolymer, and w_{tol} , the weight fraction of toluene in the mixed solvent.
- (21) Provencher, S. W. *Comput. Phys. Commun.* **1982**, *27*, 229.
- (22) von Meerwall, E. D. *Adv. Polym. Sci.* **1983**, *54*, 1.
- (23) Stilbs, P. *Prog. NMR Spectrosc.* **1987**, *19*, 1.
- (24) Chu, B.; Wu, D. *Macromolecules* **1987**, *20*, 1606.
- (25) Born, M.; Wolf, E. *Principles of Optics*, 6th ed.; Pergamon: Oxford, 1983.
- (26) Lodge, T. P.; Bates, F. S.; Pan, C.; Maurer, W.; Jin, X.; Zhao, J. *Bull. Am. Phys. Soc.* **1995**, *40*, 728.
- (27) Yamakawa, H. *Modern Theory of Polymer Solutions*; Harper & Row: New York, 1971.
- (28) Rey, A.; Freire, J. J. *J. Chem. Phys.* **1994**, *101*, 2455.
- (29) Adler, R. S.; Freed, K. F. *Macromolecules* **1978**, *11*, 1058.
- (30) Muthukumar, M.; Freed, K. F. *Macromolecules* **1978**, *11*, 843.
- (31) Muthukumar, M. *J. Chem. Phys.* **1983**, *79*, 8.
- (32) Amelar, S.; Eastman, C. E.; Morris, R. L.; Smeltzly, M. A.; Lodge, T. P.; von Meerwall, E. D. *Macromolecules* **1991**, *24*, 3505.
- (33) Landry, C. J. T. Ph.D. Thesis, University of Wisconsin, 1985.
- (34) Lodge, T. P.; Schrag, J. L. *Macromolecules* **1982**, *15*, 1376.
- (35) Martel, C. J. T.; Lodge, T. P.; Dibbs, M. G.; Stokich, T. M.; Sammler, R. L.; Carriere, C. J.; Schrag, J. L. *Faraday Symp. Chem. Soc.* **1983**, *18*, 173.
- (36) Patel, S. S.; Takahashi, K. M. *Macromolecules* **1992**, *25*, 4382.
- (37) Zimm, B. H. *J. Chem. Phys.* **1956**, *24*, 269.
- (38) Ferry, J. D. *Viscoelastic Properties of Polymers*, 3rd ed.; Wiley: New York, 1980.
- (39) Olvera de la Cruz, M. *J. Chem. Phys.* **1989**, *90*, 1995.
- (40) Fredrickson, G. H.; Leibler, L. *Macromolecules* **1989**, *22*, 1238.
- (41) Jian, T.; Anastasiadis, S. H.; Fytas, G.; Adachi, K.; Kotaka, T. *Macromolecules* **1993**, *26*, 4706.
- (42) Fredrickson, G. H.; Helfand, E. *J. Chem. Phys.* **1987**, *87*, 697.
- (43) Bates, F. S.; Rosedale, J. H.; Fredrickson, G. H. *J. Chem. Phys.* **1990**, *92*, 6255.

MA946123J